Radioactivity of neutron deficient isotopes in the region $N>82>Z$

R. D. Page,[1,*] P. J. Woods,[1] R. A. Cunningham,[2] T. Davinson,[1] N. J. Davis,[1] A. N. James,[3] K. Livingston,[1,†] P. J. Sellin,[1,‡] and A. C. Shotter[1]

[1]*Department of Physics and Astronomy, University of Edinburgh, The King's Buildings, Edinburgh EH9 3JZ, United Kingdom*
[2]*CCLRC Daresbury Laboratory, Warrington WA4 4AD, United Kingdom*
[3]*Oliver Lodge Laboratory, University of Liverpool, P.O. Box 147, Liverpool L69 3BX, United Kingdom*

(Received 12 October 1995)

The α decay characteristics of 88 decay lines emanating from 74 isotopes are presented, including new α decay lines identified in the neutron deficient nuclides ^{158}Ta (E_α=5969±8 keV, $t_{1/2}$=46±4 ms), ^{159}Ta (E_α=5516±5 keV, $t_{1/2}$=1100±100 ms), ^{160}Ta (E_α=5313±5 keV, $t_{1/2}$=1700±200 ms), ^{168}Ir (E_α=6323 ±8 keV, $t_{1/2}$=161±21 ms, b_α=82±14%), and ^{170}Ir (E_α=6083±11 keV, $t_{1/2}$=830±300 ms, b_α=36 ±10%). Their correlations with other decay lines are discussed. The alpha decay of a high-spin isomer in ^{157}Ta has been discovered, with an energy of 7744±8 keV and a half-life of 1.7±0.1 ms, while the half-life of the corresponding isomeric alpha decay line of ^{158}W has been measured for the first time as 160±50 μs. First half-life and branching ratio measurements are also reported for the 5454±4 keV ^{156}Lu line ($t_{1/2}$=494 ±12 ms), ^{162}Re (b_α=85±9%), ^{163}Os ($t_{1/2}=12^{+11}_{-7}$ ms), ^{166}Ir ($t_{1/2}$=12±1 ms), ^{167}Ir ($t_{1/2}$=34±4 ms), the 6227 ±15 keV ^{168}Ir line ($t_{1/2}$=125±40 ms), and ^{171}Ir (b_α=58±11%). New decay measurements for the proton emitter ^{156}Ta (E_p=1108±8 keV, $t_{1/2}$=375±54 ms, b_p=4.2±0.9%; E_p=1007±5 keV, $t_{1/2}$=144±24 ms) are presented. All energies have been measured using a consistent energy calibration procedure for protons and α particles.

PACS number(s): 23.60.+e, 21.10.Tg, 23.50.+z, 27.70.+q

I. INTRODUCTION

Proton and α radioactivity represents a unique source of information on the spectroscopy of extremely neutron-deficient nuclei in the region $N>82>Z$. Detailed nuclear structure information on single-particle levels can be determined from decays of ground and isomeric states, while decay Q values provide a stringent test for mass models, helping to define the location of the proton drip line and hence the experimental limits to nuclear existence.

In-flight separation coupled with implantation detection systems has proved to be an extremely powerful tool for studying the radioactivity of these exotic nuclei produced in heavy-ion fusion-evaporation reactions. The separation is fast (~1 μs), which means that the decays of short-lived nuclides can be studied, and is independent of the chemistry of the reaction products. Consequently, the decays of a very wide range of nuclides can be studied simultaneously using a sensitive implantation detection system to analyze the complex decay particle spectra.

In an extensive program of experiments to search for new cases of proton radioactivity at the Daresbury Laboratory Nuclear Structure Facility [1–6], a wealth of α decay data was obtained. The data presented in this paper were obtained from eight reactions studied in five different experiments in this program (see Table I).

II. EXPERIMENTAL DETAILS

The technique employed in the present experiments has been described in detail elsewhere [7]. The nuclides of interest are produced in heavy-ion fusion-evaporation reactions and separated in flight according to their mass to charge state ratio A/q using a recoil mass separator (RMS). The selected ions are implanted at the focal plane of the RMS into a ~65-μm-thick double-sided silicon strip detector (DSSSD) comprising 48 300-μm-wide strips on each face, which provide position information in two dimensions. The DSSSD is used to measure decay particle energies [resolution ≲20 keV full width at half maximum (FWHM)] and to correlate causally related events using the (x,y) position information and a time measurement recorded with each event.

Special care must be taken when measuring the decay properties of implanted nuclides [8]. For the energy measurements in the present work, corrections have been applied to take into account the pulse height defect for α particles and protons in silicon [9], the contribution of the recoiling daughter nucleus to the energy signal [10], and the nonlinear response of silicon detectors for low-Z ions [11]. Using this procedure, a consistent energy calibration for both protons and alpha particles is obtained. Half-lives and branching ratios can be measured by correlating causally related events, but it is essential to allow for accidental correlations of random events [12]. This is particularly important for half-life measurements of relatively long-lived first generation decays, where correlations with the preceding implantation event are made and there is no guarantee that this is necessarily the true parent ion. For branching ratio measurements, allowance must be made for the decay particles which escape from the detector without depositing their full energy [8], while the strip architecture also leads to a small correction (~2%) to branching ratios since for clean spectra only

*Present address: Oliver Lodge Laboratory, University of Liverpool, Liverpool L69 3BX, United Kingdom.
†Present address: Department of Physics and Astronomy, University of Glasgow, Glasgow, United Kingdom.
‡Present address: Department of Physics, University of Sheffield, Sheffield S3 7RH, United Kingdom.

TABLE I. Summary of reactions studied in the present work. Beam energies are for the front of the target.

Beam species	Beam energy (MeV)	Average beam current (pnA)	Target isotope	Nominal target thickness (mg cm^{-2})	Compound nucleus	Length of run (h)
^{58}Ni	290	6	^{102}Pd	1.0	^{160}W	28
^{58}Ni	300	2	^{106}Cd	0.7	^{164}Os	26
^{58}Ni	297	5	^{112}Sn	0.9	^{170}Pt	3.5
^{58}Ni	329	4	^{112}Sn	0.9	^{170}Pt	43
^{70}Ge	309	2	^{106}Cd	0.7	^{176}Hg	18
^{70}Ge	354	2	^{106}Cd	0.7	^{176}Hg	46
^{70}Ge	316	2	^{112}Sn	0.9	^{182}Pb	12
^{70}Ge	360	2	^{112}Sn	0.9	^{182}Pb	11

events with signals in one strip per face are generally considered.

The energy calibration for data obtained using the reaction ^{58}Ni + ^{102} Pd was based on the energy of the ^{147}Tm ground state proton decay line [13] (produced using a ^{92}Mo target as part of the same experiment) and the energies of the α decay lines of ^{150,151}Dy, ^{151m,152m}Ho, and ^{152}Er [14]. Calibrations for the remaining ^{58}Ni-induced reactions were obtained by matching common α decay line centroids to these data. The energies of the α decay lines from ^{168,170}Os, ^{171,172,174,175,177,178}Pt, ^{179} Au, and ^{180}Hg [14] were used for calibrating the ^{70}Ge-induced reactions, which were studied in a single experiment.

III. RESULTS AND DISCUSSION

The results of α decay measurements from the present work are summarized in Table II and compared with literature values where available. Of these decay lines, 8 are new, while for the remaining 80 lines, 6 half-lives and 2 branching ratios have been measured for the first time. The present measurements generally agree well with those from the literature and more precise values have been obtained in many cases. Several of the nuclides studied exhibit fine structure and Table III shows the Q-value differences measured in these cases. The new decay measurements and other points of interest arising from the present work are discussed in the following sections.

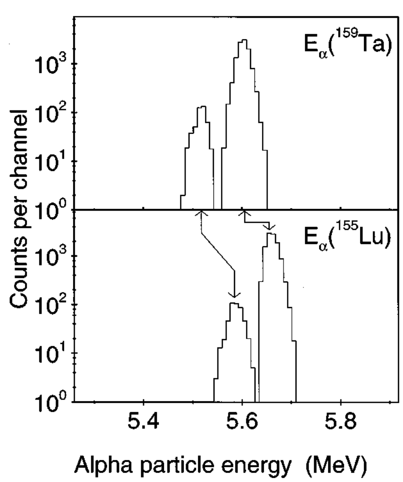

FIG. 1. Projections of α decay lines of ^{159}Ta (upper spectrum) and ^{155}Lu (lower spectrum), with the arrows indicating which lines are correlated. The higher-energy ^{155}Lu line at 5655$\pm$5 keV is correlated with the previously known 5599$\pm$5 keV ^{159}Ta line, while the 5584$\pm$5 keV line is correlated with a new ^{159}Ta line which has an energy of 5516$\pm$5 keV.

A. Fine structure of the ^{153}Tm α decay line

Evidence that the ^{153}Tm α decay line is a doublet was first reported by Schardt *et al.* [19], who determined an energy difference of 7$\pm$4 keV for the two components. The relative energies of the α decaying $\pi h_{11/2}$ and $\pi s_{1/2}$ levels were determined from the fine structure in ^{153}Tm α decay [60] and from detailed decay schemes for ^{149}Ho [61] and ^{153}Tm [20]. From studies of the decays of the ^{157}Lu and ^{153}Tm decay lines, Lewandowski *et al.* deduced an energy difference of 10$\pm$3 keV for the ^{153}Tm lines [62].

In data obtained in the reactions of 300 MeV ^{58}Ni + ^{106}Cd and 329 MeV ^{58}Ni+^{112}Sn, α decays of the $\pi h_{11/2}$ level in ^{157}Lu were cleanly correlated with decays of the corresponding level in ^{153}Tm. This component of the ^{153}Tm doublet was thus isolated and an energy of 5112$\pm$5 keV was determined. The α decay of the low-spin level in ^{157}Lu [26,62] was not identified in the present data, and so it was not possible to correlate this decay line to isolate the $\pi s_{1/2}$ line from ^{153}Tm. However, the α decay of ^{157}Hf produces ^{153}Yb, which in turn β decays to populate both levels in ^{153}Tm [20]. Correlations of ^{157}Hf and ^{153}Tm α decays yielded a peak which is an admixture of the two components and has a centroid 6$\pm$3 keV lower than the pure $\pi h_{11/2}$ decay line. This provides further evidence for the doublet structure of ^{153}Tm, but the energy difference determined in the present work can only be regarded as a lower limit.

B. α decay fine structure in neutron-deficient tantalum isotopes

The α decays of ^{163}Re and ^{159}Ta leading to the α decay of ^{155}Lu were first reported by Hofmann *et al.* [8], who observed a single decay line for each nuclide. However, three α decay lines are now known for ^{155}Lu [28]: The highest-energy line represents the decay of a $[\pi h_{11/2} \nu f_{7/2} h_{9/2}]25/2^-$ high-spin isomeric state (Sec. III G), while the two other lines with energies of 5584$\pm$5 keV and 5655$\pm$5 keV originate from the ground state and a low-energy isomer. These latter two decay lines are believed to represent transitions between levels with $d_{3/2}(s_{1/2})$ or with $h_{11/2}$ proton configu-

TABLE II. Summary of α decay measurements from the present work compared with literature values where available.

	E_α (keV)		$t_{1/2}$ (ms)		b_α (%)	
Nuclide	This work	Literature[a]	This work	Literature[a]	This work	Literature[a]
^{149}Tb	3973±4	3967±2 [14]		$(1.4825\pm0.0009)\times10^{7}$ [15]		16.7±1.7 [15]
^{151}Ho	4521±5	4522±2 [14]		35200±1000 [16]		22±3 [17]
^{153}Er	4674±4	4677±2 [14]		37100±200 [16]		53±3 [18]
^{153}Tm	5112±5	5111±2 [14]		1480±10 [19]		91±3 [20]
^{156}Yb	4687±4	4688±7 [8,18]		24800±800 [18,21]		12±2 [8,21]
^{155}Yb	5202±4	5200±4 [14]	1800±20	1740±50 [8,16,18,22]		88±4 [8,22]
^{154}Yb	5331±4	5331±2 [14]	409±2	417±16 [8,18,23]	92±2	92.9±1.4 [8,23]
^{157}Lu	4997±4	5001±3 [14]		4900±140 [24–27]		6±2 [8]
^{156}Lu	5454±4	5450±10 [8]	494±12[b]	∼500 [8]		
^{156}Lu	5565±4	5567±5 [14]	198±2	180±20 [8]	98±9	100±25 [8]
^{155}Lu	5584±5	5578±4 [22,28]	136±9	140±20 [26]		
^{155}Lu	5655±5	5650±3 [8,22,28]	70±1	68±5 [8,26]	81±9	79±4 [8]
^{155}Lu	7390±5	7396±8 [8,28]	2.71±0.03	2.62±0.07 [8,29]		
^{160}Hf	4778±6	4780±3 [14]		13.0±1.5 [27]		2.3±0.6 [8]
^{159}Hf	5098±5	5093±3 [14]	5200±100	5670±440 [24,27]	16±5	14±1 [8,30]
^{158}Hf	5269±4	5267±4 [14]	2850±70	2900±190 [8,24]	45±3	46±3 [8]
^{157}Hf	5729±4	5731±5 [14]	115±1	110±6 [8]	95±5	91±7 [8]
^{156}Hf	5873±4	5878±10 [8]	23±1	25±4 [8]	100±6	100±19 [8]
^{156}Hf	7782±4	7804±15 [8]	0.52±0.01	0.49±0.02 [8,28,29]		
^{161}Ta	5140±7	5148±5 [14]	4900±800	2870±120 [27,31]		
^{160}Ta[b]	5313±5		1700±200			
^{160}Ta	5413±5	5412±5 [14]	1550±40	1500±170 [27,31]		
^{159}Ta[b]	5516±5		1100±100			
^{159}Ta	5599±5	5601±6 [8]	544±16	570±180 [8]	73±14	80±5 [8]
^{158}Ta[b]	5969±8		46±4			
^{158}Ta	6046±4	6051±6 [8]	35±1	36.8±1.6 [8]	99±13	93±6 [8]
^{157}Ta	6213±4	6219±10 [8]	4.3±0.1	5.3±1.8 [8]	95±12	100±23 [8]
^{157}Ta[b]	7744±8		1.7±0.1			
^{164}W	5148±6	5150±2 [14]		6020±320 [8,32,33]	5±1	2.6±1.7 [8]
^{163}W	5383±6	5384±2 [14]	3000±1300	2800±170 [8,32]	13±2	39±4 [8,30]
^{162}W	5541±5	5534±3 [14]	1200±100	1390±40 [8]	44±2	46±4 [29]
^{161}W	5775±5	5776±5 [14]	409±18	410±40 [8]	73±3	82±26 [29]
^{160}W	5912±5	5920±10 [8]	91±5	81±15 [29]	87±8	94±40 [29]
^{159}W	6292±5	6299±6 [29]	8.2±0.7	7.3±2.7 [29]	92±23	200±120 [29]
^{158}W	6442±30	6442±21 [8,28]	$0.9^{+0.4}_{-0.3}$	0.9±0.3 [28]		
^{158}W	8291±24	8280±30 [28]	0.16±0.05[b]	0.01-1 [28]		
^{166}Re	5533±10	5515±4 [34–36]		2120±380 [34,36]		
^{165}Re	5518±5	5506±10 [29]	1900±300	2400±600 [29]		13±3 [29]
^{164}Re	5784±7	5778±10 [8]	380±160	880±240 [29]		
^{163}Re	5918±7	5918±6 [8]	219±23	260±40 [8]	82±11	64±18 [29]
^{162}Re	6123±6	6119±6 [8]	66±7	100±30 [8]	85±9[b]	
^{161}Re	6265±6	6279±10 [8]	14±2	10^{+15}_{-5} [8]		
^{160}Re[b]	6543±16		$0.79^{+0.19}_{-0.13}$		9±5	
^{172}Os	5106±10	5102±6 [37,38]		19140±820 [37,38]		1.1±0.2 [38]
^{171}Os	5248±9	5245±5 [34,38–40]		8210±190 [34,38,39]		1.8±0.2 [38,40]
^{170}Os	c	5407±4 [14]	9000±1000	7310±155 [38,39,41,42]	8.6±0.6	8.5±0.7 [38,41]
^{169}Os	5576±8	5575±6 [38,43]	3600±200	3340±110 [34,38,41,42]	11±1	11.7±0.9 [38,41]
^{168}Os	c	5676±4 [14]	2100±100	2100±60 [30,34,41,42]	40±3	49±3 [41]
^{167}Os	5853±5	5836±2 [14]	840±70	780±110 [29,41,44]	49±7	68±8 [29,41]
^{166}Os	6000±6	5985±6 [29,44]	220±7	202±15 [29,44,45]		72±13 [29]
^{165}Os	6188±7	6176±9 [29,30]	71±3	72±8 [29,45]		100±40 [29]
^{164}Os	6321±7	6320±20 [29]	21±1	41±20 [29]		100±70 [29]

TABLE II. (*Continued*).

Nuclide	E_α (keV)		$t_{1/2}$ (ms)		b_α (%)	
	This work	Literature[a]	This work	Literature[a]	This work	Literature[a]
^{163}Os	6512±19	6510±30 [29]	12^{+11}_{-7} [b]			
^{173}Ir	5681±13	5672±5 [14]	2400±900	2470±45 [46,47]	7±2	2.02±0.08 [48]
^{172}Ir	5822±12	5823±6 [14]		2050±70 [34,47]		
^{171}Ir	5945±11	5920±4 [14]	1300±200	1470±80 [30,34,46]	58±11[b]	
^{170}Ir	6003±10	6025±5 [14]		1070±120 [34,44]		
^{170}Ir[b]	6083±11		830±300		36±10	
^{169}Ir	6119±9	6126±5 [14]	308±22	400±90 [30,34]	72±13	83^{+17}_{-42} [49]
^{168}Ir	6227±15	6250±5 [30,35]	125±40[b]			
^{168}Ir[b]	6323±8		161±21		82±14	
^{167}Ir	6410±11	6386±10 [29]	34±4[b]			
^{166}Ir	6556±11	6541±20 [29]	12±1[b]			
^{176}Pt	5741±8	5751±2 [14]	6700±700	6330±150 [50]	42±4	40±2 [18,51]
^{175}Pt	c	5960±3 [14]	2400±300	2520±80 [50]	56±5	55±5 [40]
^{174}Pt	c	6038±4 [14]	890±20	880±10 [41,52]	67±6	83±5 [40]
^{173}Pt	6225±9	6205±3 [14]	376±11	342±14 [41,52]	83±14	84±6 [40]
^{172}Pt	c	6314±4 [14]	96±3	106±7 [41,49,52]		94±32 [49]
^{171}Pt	c	6453±3 [14]	43±3	31±5 [41,49,52]		
^{169}Pt	6698±23	6678±15 [29]	5±3	$2.5^{+2.5}_{-1.0}$ [29]		
^{179}Au	c	5847±5 [14]	3300±1300	7100±300 [53]		22.0±0.9 [48]
^{178}Au	5886±9	5850±20 [48]		2600±500 [54]		
^{177}Au	6118±9	6110±10 [55]	1300±200	1230±60 [45,55]		
^{177}Au	6154±10	6150±10 [55]		1230±60 [45,55]		
^{175}Au	6438±9	6438±7 [49,55]	185±30	200±22 [56]		94^{+6}_{-25} [56]
^{174}Au	6544±10	6541±9 [49,56]	171±29	120±20 [56]		
^{174}Au	6637±13	6626±10 [49]		120±20 [49]		
^{173}Au	6749±9	6731±9 [49,56]	15±2	59^{+45}_{-18} [56]		
^{172}Au[b]	6878±9		6.3±1.5			
^{181}Hg	5986±13	6005±4 [14]		3600±30 [51]		26±4 [40]
^{180}Hg	c	6119±5 [14]	2600±800	2800±200 [57]		48±4 [57]
^{179}Hg	6275±9	6285±5 [14]	929±114	1090±400 [58]		55±25 [59]
^{178}Hg	6428±9	6430±6 [40]	287±23	255±19 [40,45]		
^{177}Hg	6577±9	6580±8 [40]	114±15	134±5 [40,45]		
^{176}Hg	6750±20	6761±9 [49,56]	18±10	34^{+18}_{-9} [56]		
^{175}Hg	6909±24	6869±14 [49,56]	8±8	20^{+40}_{-13} [56]		
^{179}Tl	6568±18	6560±20 [56]	430±350	160±50 [49]		
^{179}Tl	7201±20	7200±10 [49]	$0.7^{+0.6}_{-0.4}$	1.4±0.5 [56]		

[a]Literature values are error-weighted averages of values given in references supplied.
[b]New decay line or new decay data.
[c]Used as a calibration line ^{70}Ge-induced reaction data.

rations, respectively, which are very close in energy in both parent and daughter nuclei [63].

Both of these low-energy decay lines were identified in the reaction 300 MeV ^{58}Ni + ^{106}Cd. The 5655 keV line was found to be correlated with the 5599±5 keV line of ^{159}Ta, in accordance with earlier results [8], while the 5584 keV line was correlated with a new decay line having an energy of 5516±5 keV and a half-life of 1.1±0.1 s (Fig. 1). The 5599 keV line is produced more strongly than the line at 5516 keV, suggesting it has a $\pi h_{11/2}$ configuration; the ^{155}Lu line with which it is correlated also has a stronger direct production rate in the 290 MeV ^{58}Ni+^{102}Pd reaction and has been assigned as a $\pi h_{11/2}$ configuration using a similar argument [63]. Further evidence that the decays proceed between levels based on $\pi h_{11/2}$ proton orbitals comes from the reduced α decay width [64] of 1.25±0.24 relative to ^{212}Po for the 5599 keV line based on the present measurements. The new, weaker 5516 keV ^{159}Ta line would then represent the $\pi d_{3/2}$ (or $\pi s_{1/2}$) configuration and is correlated with the line assigned to the corresponding low-spin proton configuration in ^{155}Lu.

Two α decay lines are also known for ^{156}Lu [8] and both were observed as daughter activities in the 300 MeV ^{58}Ni + ^{106}Cd reaction. Correlations with preceding decays reveal a

TABLE III. Energy and Q-value differences for nuclides for which more than one α decay line was measured in the present work. The uncertainties in these differences are reduced because the uncertainty in the offset of the energy calibration cancels.

Nuclide	Energy difference (keV)	Q-value difference (keV)
^{156}Lu	112 ± 1	115 ± 1
^{155}Lu	71 ± 3	73 ± 3
^{160}Ta	100 ± 4	103 ± 4
^{159}Ta	83 ± 3	85 ± 3
^{158}Ta	77 ± 7	79 ± 7
^{170}Ir	79 ± 15	81 ± 15
^{168}Ir	96 ± 16	98 ± 16
^{177}Au	36 ± 6	36 ± 6
^{174}Au	93 ± 11	96 ± 11
^{179}Tl	633 ± 24	648 ± 24

new decay line with an energy of 5313 ± 5 keV and a half-life of 1.7 ± 0.2 s, which is correlated with the 5454 ± 4 keV ^{156}Lu line, while the 5413 ± 5 keV ^{160}Ta line is correlated with the 5565 ± 4 keV ^{156}Lu line (Fig. 2). The half-life of the 5454 keV ^{156}Lu line was measured for the first time as 494 ±12 ms and, assuming a 100% branching ratio, this would correspond to a reduced width of 0.94 ± 0.02.

The 290 MeV ^{58}Ni+^{102}Pd data were also analyzed for evidence of fine structure in the decays of ^{157,158}Ta. No conclusive evidence was found regarding fine structure in ^{157}Ta, but a new decay line at an energy of 5969 ± 8 keV and having a half-life of 46 ± 4 ms was identified in the $A=158$ region of the DSSSD (Fig. 3). Correlations indicated that this decay was followed by the α decay of ^{154}Yb, but these correlated daughter α decays were delayed, having a half-life significantly longer than the value of 409 ± 2 ms deduced from correlations with ^{158}Hf which feeds ^{154}Yb directly. This would be consistent with the decay of a ^{158}Ta level to

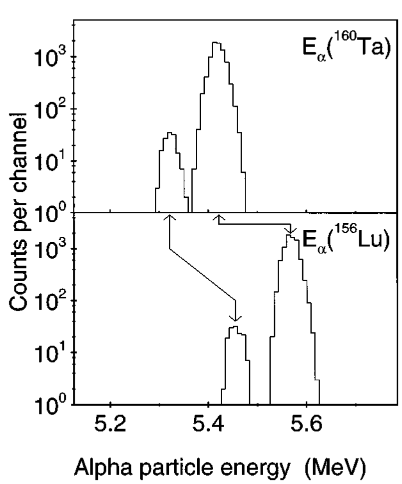

FIG. 2. Projections of α decay lines of ^{160}Ta (upper spectrum) and ^{156}Lu (lower spectrum), with the correlations indicated by arrows. The higher-energy ^{156}Lu line at 5565 ± 4 keV is correlated with the previously known 5413 ± 5 keV ^{160}Ta line, while the 5454 ±4 keV line is correlated with a new ^{160}Ta line which has an energy of 5313 ± 5 keV.

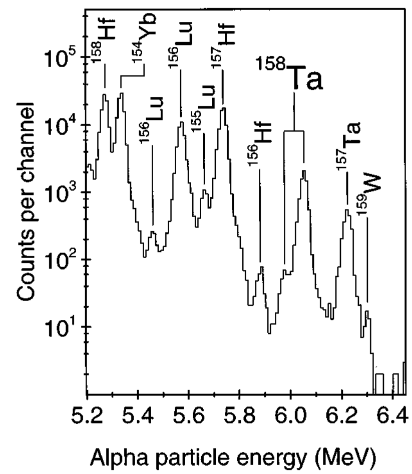

FIG. 3. Energy spectrum observed in the reaction 290 MeV ^{58}Ni + ^{102} Pd, with a wide $A=158$ mass gate. Assignments to main α decay lines are given, including ^{158}Ta for which a new line at an energy of 5969 ± 8 keV has been identified in the present work, in addition to the previously known 6046 ± 4 keV line.

^{154}Lu ($t_{1/2}=960\pm100$ ms [29]) which then β decays to the α emitter ^{154}Yb. A reduced α decay width of 0.67 ± 0.06 is calculated for this decay line, assuming a branching ratio of 100%. This compares with a reduced width of 0.45 ± 0.06 for the 6046 ± 4 keV ^{158}Ta line, based on the present measurements.

C. α decays of $^{162-164}$Re

The α decays of $^{162-164}$Re were identified in the reactions ^{58}Ni+^{112}Sn and in each case a single decay line was observed. The 6123 ± 6 keV ^{162}Re line was found to be correlated with the 6046 ± 4 keV line from ^{158}Ta, while the 5918 ±7 keV ^{163}Re line correlated with the 5599 ± 5 keV ^{159}Ta line, in accordance with Ref. [8]. No correlations leading to the new 5969 ± 8 keV ^{158}Ta or 5516 ± 5 keV ^{159}Ta lines were observed. Hofmann *et al.* reported no correlations with the ^{164}Re decay line [8], but in the present data, this decay line was found to be correlated with the new 5313 ± 5 keV ^{160}Ta line, rather than the previously known 5413 ± 5 keV line. This is in striking contrast with the two lighter rhenium isotopes, which correlate with the more strongly produced tantalum line in each case. It is interesting to compare this case with that of ^{160}Re, for which only decays of the $\pi d_{3/2}$ level have been observed [1].

D. α decays of iridium isotopes

The α decays of the isotopes ^{166,167}Ir have been assigned through correlations with the α decays of their rhenium daughters, but only lower limits of 5 ms were determined for their half-lives [29]. In both reactions using beams of ^{58}Ni ions to bombard ^{112}Sn targets, the assignments of ^{166,167}Ir α decays were confirmed by the observation of α decay lines with energies of 6556 ± 11 keV and 6410 ± 11 keV in the $A=166$ and 167 regions of the RMS focal plane, respectively, and first half-life measurements of 12 ± 1 ms and 34 ±4 ms were obtained for these decay lines. Assuming α

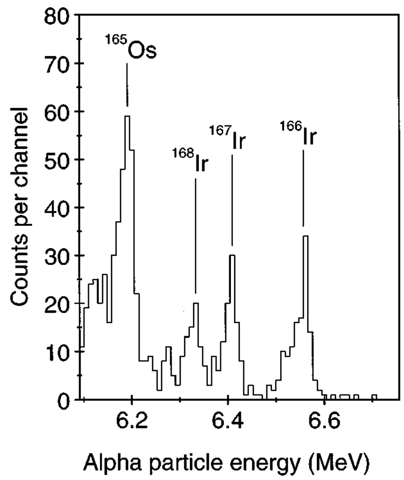

FIG. 4. High-energy part of the spectrum observed in the reaction 297 MeV ^{58}Ni + ^{112}Sn. Assignments to the strongest α decay lines are given. The low-energy tailing on the ^{166}Ir peak is a result of radiation damage in the $A=166$ region sustained by this DSSSD in an earlier experiment.

decay branching ratios of 100% in each case, these half-lives correspond to reduced decay widths of 0.81 ± 0.07 for ^{166}Ir and 0.92 ± 0.11 for ^{167}Ir. The ^{166}Ir decay line was found to be correlated with the 6123 ± 6 keV ^{162}Re line, the branching ratio of which was measured for the first time as 85 ± 9 %, and from this a reduced α decay width of 0.73 ± 0.11 relative to ^{212}Po was deduced. Similarly, the ^{167}Ir decay line and the 5918 ± 7 keV ^{163}Re line were found to be correlated. Both of these lines are produced directly and correlate with the 5599 ±5 keV ^{159}Ta and 5655 ± 5 keV ^{155}Lu lines, which are assigned as $\pi h_{11/2}$ levels based on their production yields, which suggests that these are also $\pi h_{11/2}$ levels. This conclusion is supported by the reduced α decay widths of the correlated decays in this chain.

A 6.22 MeV α decay line has previously been assigned to the isotope ^{168}Ir on the basis of its excitation function, but no

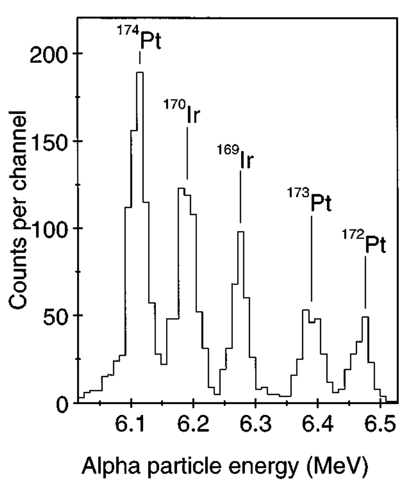

FIG. 5. Part of the energy spectrum observed in the reaction 354 MeV ^{70}Ge + ^{106}Cd, gated on the region $A=169$–170. The platinum isotopes appear in this region of the RMS focal plane in an ionic charge state one greater than the iridium isotopes and hence have a similar A/q ratio.

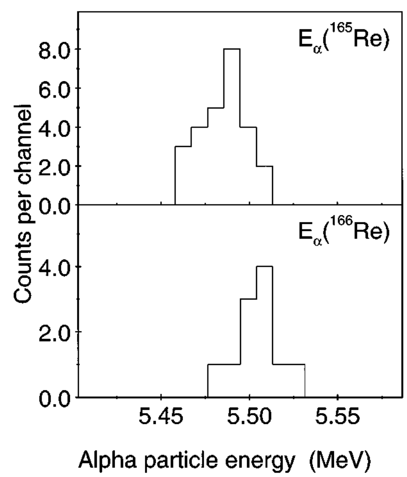

FIG. 6. Projections of α decays of ^{165}Re (upper spectrum) and ^{166}Re (lower spectrum), which are correlated with the ^{169}Ir and ^{170}Ir lines shown in Fig. 5, respectively.

half-life measurement was reported [30,35]. In the reaction 297 MeV ^{58}Ni + ^{112}Sn, an $A=168$ decay line was observed at an energy of 6323 ± 8 keV, too high to be consistent with the 6.22 MeV line (Fig .4). The half-life of this decay line was determined as 161 ± 21 ms. It was not found to be correlated with any daughter activity but was correlated with the α decays of the new isotope ^{172}Au in the reaction 354 MeV ^{70}Ge + ^{106}Cd [3]. This new decay line is therefore assigned as the decay of ^{168}Ir. A reduced α decay width of 0.32 ±0.07 was deduced for this decay line, which is significantly lower than the values for neighboring isotopes, perhaps indicating a hindered α decay.

Another, weaker decay line with an energy of 6227 ± 15 keV and a half-life of 125 ± 40 ms was also identified. However, owing to the poor statistics in the present data, it was not possible to prove unambiguously whether this was an $A=168$ or 169 activity; nor were any correlations observed. The energy of this line is consistent with that measured previously for the line assigned as ^{168}Ir [30,35], and so this decay line is tentatively assigned as a second decay line from ^{168}Ir.

The α decay of ^{171}Ir has been previously identified with an energy of 5920 ± 4 keV and a half-life of 1.47 ± 0.08 s. This decay line was observed in the reaction 354 MeV ^{70}Ge + ^{106}Cd as the daughter of ^{175}Au α decays. A correlation analysis yielded a first branching ratio measurement of $58\pm$ 11% for this nuclide, which corresponds to a reduced decay width of 0.75 ± 0.18, using the energy and half-life measured in the present work.

E. α decays of ^{165}Re and ^{166}Re

Considerable controversy has arisen from different assignments to activities observed at ~5.5 MeV. A 5495 ± 10 keV decay line was first reported by Schrewe *et al.* and attributed to the α decay of ^{166}Re on the basis of excitation function arguments [34]. Subsequently, Hofmann *et al.* found ^{169}Ir α decays to be correlated with a 5506 ± 10 keV daughter activity and assigned it to ^{165}Re [29]. An excitation function analysis by Della Negra *et al.* [35] identified a 5527 ±4 keV acitivity as the ^{166}Re decay line observed by

Schrewe *et al.*, while Meissner *et al.* [36] later observed a 5501±13 keV activity for which an assignment to ^{166}Re was favored, although the possibility of ^{165}Re could not be eliminated. More recently, Hild *et al.* [38] reported a 5508±8 keV activity observed in coincidence with γ rays and tungsten K x rays, which was interpreted as a fine structure component in the α decay of ^{169}Os, rather than the decay of a rhenium isotope. However, from cross bombardments Schrewe *et al.* argued that the activity they observed could not be an iridium or osmium α emitter.

In the reaction 354 MeV ^{70}Ge + ^{106}Cd, approximately 600 ^{170}Ir and 300 ^{169}Ir events could be cleanly identified (Fig. 5). Correlating these events with subsequent daughter decays revealed decay lines at 5533±10 keV and 5518±5 keV (Fig. 6), which are therefore assigned to ^{166}Re and ^{165}Re, respectively. This confirms the assignment to ^{165}Re on the basis of correlations by Hofmann *et al.* and demonstrates that ^{166}Re has a comparable α decay energy; so the assignments of activities to this isotope could also be correct.

F. α decays of ^{174,177}Au

In the reaction 309 MeV ^{70}Ge + ^{106}Cd, two α decay lines assigned to ^{174}Au by Schneider [49] were identified. The more intense 6544±10 keV line was found to be correlated with a previously unobserved ^{170}Ir line at an energy of 6083 ±11 keV, which has a half-life of 830±300 ms and a branching ratio of 36±10 %. However, no further correlations of this decay chain with ^{166}Re α decays were identified, whereas the previously known lower-energy ^{170}Ir line is correlated with the ^{166}Re line (see above). The existence of correlations with the weaker 6637±13 keV ^{174}Au line could not be established owing to the low number of events. The measurements for this new ^{170}Ir line indicate a reduced s-wave α decay width of 0.21±0.10 relative to ^{212}Po.

Two α decay lines are also known for ^{177}Au [45,55] and these were identified in the reactions 354 MeV ^{70}Ge + ^{106}Cd and 360 MeV ^{70}Ge + ^{112}Sn. Only the lower-energy, less intense line was found to be correlated with a daughter activity: the 5681±13 keV ^{173}Ir decay line.

G. α-decaying high-spin $N=84$ isomers

Two high-energy α decay lines were first observed in experiments using the velocity filter SHIP at GSI, with energies (half-lives) of 7408±10 keV (2.7±0.3 ms) and 7804±15 keV (520±160 μs) [8]. These decays were interpreted as α decays from a $[\pi h_{11/2}\nu f_{7/2}h_{9/2}]25/2^-$ isomer in ^{155}Lu and a $[\nu f_{7/2}h_{9/2}]8^+$ isomer in ^{156}Hf, respectively, and were found to be hindered by a factor of ~18 relative to ^{212}Po α decay, assuming $\Delta l=8$. In a subsequent experiment [28], an 8280 ±30 keV decay line was assigned to the α decay of the corresponding isomer in ^{158}W, with a half-life in the range 0.01–1 ms. The energy and half-life of the ^{155}Lu line were also remeasured as 7379±15 keV and 2.60±0.07 ms. However, no evidence could be found in either experiment for decays from a corresponding isomeric state in the $N=84$ isotone ^{157}Ta, leaving a gap in the systematics.

The α decays of these high-spin isomers were investigated in the present experiments using beams of 290 MeV ^{58}Ni ions to bombard an isotopically enriched 1-mg cm^{-2}-thick ^{102}Pd target. The relevant part of the energy spectrum is shown in Fig. 7, in which the α decay lines of the three previously observed isomers are indicated. The mass assignments of these three lines were confirmed using the direct mass information provided by the recoil separator and the half-life of the ^{158}W line was measured for the first time as 160±50 μs. Although there is no clear evidence for a separate peak corresponding to the decay of the isomer in ^{157}Ta in Fig. 7, the decay curve for the ^{156}Hf line reveals two distinct time components (Fig. 8): the stronger component corresponds to a half-life of 520±10 μs and is identified as arising from the ^{156}Hf line, while the second has a half-life of 1.7±0.1 ms and corresponds to a low-energy component in the decay line (Fig 9). This new activity is tentatively assigned to the decay of the ^{157}Ta isomer, although no direct mass assignment was possible in this case because it was unresolved in energy and mass from the much more intense ^{156}Hf line.

The data for this new line and the half-life measurement for the ^{158}W line are presented in Table IV, alongside the present results for ^{155}Lu and ^{156}Hf. Comparison of the measured half-lives with values calculated according to the method of Rasmussen [64] assuming $\Delta l=8$ and α decay branching ratios of 100% yields hindrance factors consistent with those determined for ^{155}Lu and ^{156}Hf, implying a similar decay mechanism in all four cases. The energy difference of the two ^{157}Ta α decay lines indicates that the isomer in this nuclide continues the trend of decreasing excitation energy with increasing atomic number for the $25/2^-$ and 8^+ isomers [28], indicating that the ground state of ^{157}Ta is 388 ±7 keV less bound against proton emission than the isomeric state is to decays to the 8^+ daughter level in ^{156}Hf.

H. α decay branching ratio of ^{163}W and the half-life of ^{163}Os

The branching ratio of ^{163}W was first measured by Cabot *et al.* [30], who determined a value of 36±6 % from the relative yields of ^{167}Os and ^{163}W excitation function curves, while a value of 41±5 % was determined by Hofmann *et al.* [8] from a comparison of the intensities of these α decay peaks. However, from correlations with ^{167}Os α decays in the reaction 297 MeV ^{58}Ni + ^{112}Sn the branching ratio of ^{163}W was measured as 13±2 %, which is in disagreement with the previously reported values. One possible reason for this discrepancy could be a contribution to the yield of the ^{163}W peaks in the previous work from direct production, which would serve to increase the observed branching ratio, a problem which is avoided in the present method by the use of correlations. It is interesting to note that the relative intensities of the peaks in the spectrum recorded in the reaction 280 MeV ^{63}Cu + ^{107}Ag in Ref. [30] strongly suggest a lower branching ratio closer to the present value, whereas the value determined in that work was taken from data obtained at higher bombarding energies. Adopting the average branching ratio from Refs. [8,30] and the literature values for the energy and half-life of ^{163} W from Table II, one would obtain a reduced α decay width of 3.0±0.2 relative to ^{212}Po, whereas the branching ratio from the present work would give a value of 1.0±0.2, which is in much better agreement with the reduced width systematics of tungsten isotopes [29].

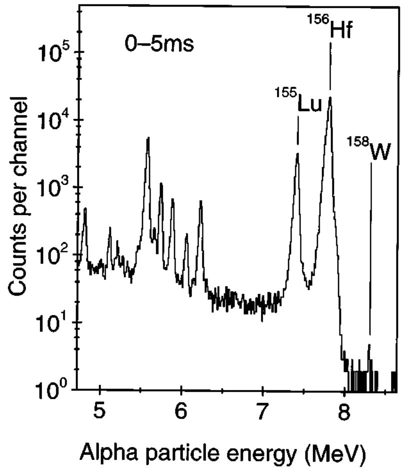

FIG. 7. Energy spectrum of decay events observed in the reaction 290 MeV ^{58}Ni + ^{102}Pd, occurring within 5 ms of an ion being implanted into the same (x,y) DSSSD position. Assignments to the α decay lines of the high-spin $N=84$ isomers are given.

The α decay of ^{163}Os has been previously identified with an energy of 6510$\pm$30 keV [29] and this decay line was observed in the reaction 329 MeV ^{58}Ni + ^{112}Sn. A first half-life measurement of 12^{+11}_{-7} ms was determined for ^{163}Os, and assuming a 100 % α decay branching ratio, this corresponds to a reduced decay width of $0.48^{+0.44}_{-0.28}$.

I. Proton radioactivity measurements

The ground state proton decay of ^{160}Re was first identified in the reaction 300 MeV ^{58}Ni + ^{106}Cd and a small number of events attributed to the α decay branch of the same level was found to be correlated with proton decays of the $\pi d_{3/2}$ level in ^{156}Ta [1]. The reaction 290 MeV ^{58}Ni + ^{102}Pd was subsequently studied in an attempt to produce ^{156}Ta directly and hence obtain better statistics by circumventing the weak ^{160}Re α decay branch. This experiment identified another proton decay line which was assigned to the decay of the $\pi h_{11/2}$ level in ^{156}Ta [5]. In the present data from this reaction, correlations with the two low-energy ^{155}Lu α decay lines reveal both the $\pi d_{3/2}$ and $\pi h_{11/2}$ proton decay lines (Fig. 10). The energy and half-life of the $d_{3/2}$ line are 1007$\pm$5 keV and 144$\pm$24 ms, which are consistent with the values determined via the α decay feeding from ^{160}Re [1]. The corresponding values for the $h_{11/2}$ line are 1108$\pm$8 keV and 375$\pm$54 ms. From the difference in energies of the two lines, the $h_{11/2}$ level is determined to be 102$\pm$7 keV above the $d_{3/2}$ ground state in ^{156}Ta. The new Q value for the $d_{3/2}$ level proton decay combined with the revised Q values from the present calibration for the ^{160}Re proton decay line (Q_p=1271$\pm$9 keV) and the α decays of ^{160}Re and ^{159}W (Table II) yield a difference of 1$\pm$18 keV for the two decay

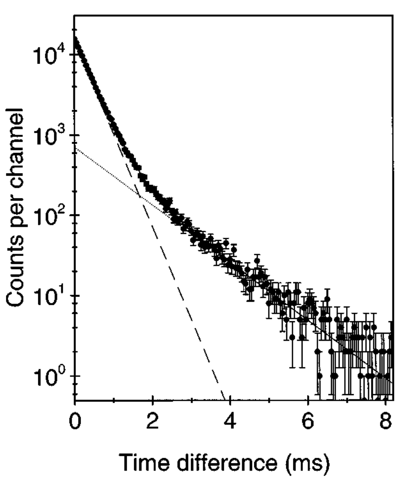

FIG. 8. Distribution of implantation-decay time differences for events in the peak labeled "^{156}Hf" in Fig. 7, which reveals two distinct components: The shorter-lived component (dashed line) is attributed to the decay of the high-spin isomer in ^{156}Hf, while the longer-lived component (dotted line) is assigned to the decay of the corresponding isomer in ^{157}Ta. The sum of these two components is represented by the solid line.

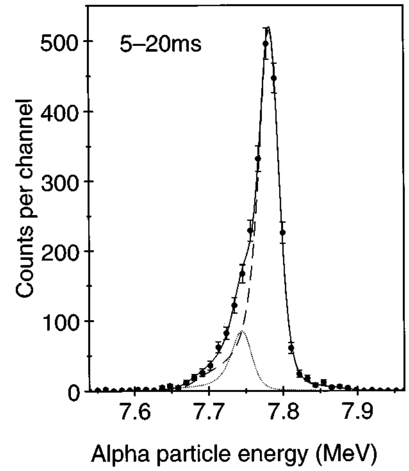

FIG. 9. Two-component fit to events in the ^{156}Hf peak in Fig. 7, occurring between 5 ms and 20 ms of ion implantation. The higher-energy component is assigned to the α decay line of the ^{156}Hf isomer, while the lower-energy component is identified as the decay line of the isomer in ^{157}Ta. The solid line represents the sum of these two components.

TABLE IV. Excitation energies and half-lives of α decaying isomers in $N=84$ isotones. The hindrance factors are the experimental half-lives divided by the results of WKB calculations assuming an angular momentum change $\Delta l=8$ and the same reduced width as for ^{212}Po. The excitation energy given for ^{155}Lu is calculated relative to the 5655 keV transition, which is presumed to populate the same final $\pi h_{11/2}$ level in ^{151}Tm. Since the relative energies of the levels emitting the 5655 keV and 5584 keV α particles are unknown, the excitation energy of the isomeric level will be uncertain if the 5584 keV line represents the decay of the ground state in ^{155}Lu.

Nuclide	Excitation energy (keV)	Measured half-life (μs)	Calculated half-life (μs)	Hindrance factor ($\Delta l=8$)
^{155}Lu	1781$\pm$2	2710$\pm$30	134$\pm$4	20$\pm$1
^{156}Hf	1959$\pm$1	520$\pm$10	28$\pm$1	19$\pm$1
^{157}Ta	1571$\pm$7	1700$\pm$100	76$\pm$4	22$\pm$2
^{158}W	1897$\pm$39	160$\pm$50	7$\pm$1	23$\pm$8

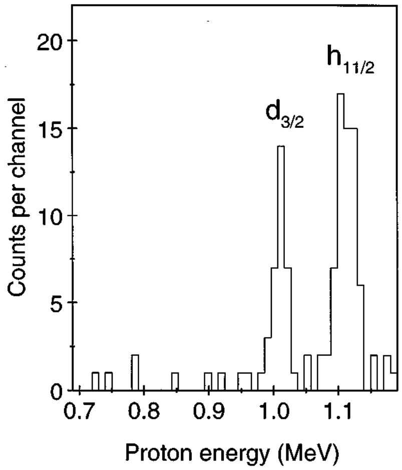

FIG. 10. Energy spectrum of correlated ^{156}Ta proton decay events observed in the reaction 290 MeV ^{58}Ni + ^{102} Pd. Different time conditions were applied for correlations with the daughter α decay lines of ^{155}Lu: For the 5655 keV line the time gates were 10 ms to 2 s between implantation and proton decay and 200 ms to 2 s between proton decay and α decay, while for the 5584 keV line the corresponding gates were 30 ms to 2 s and 300 ms to 2 s, respectively. The peaks are labeled with the proton orbitals assigned from comparisons of measured partial proton decay half-lives with calculated values.

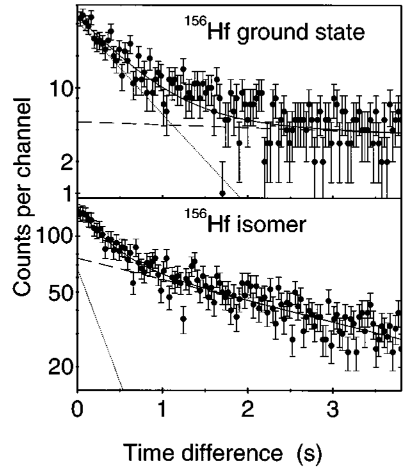

FIG. 11. Tails of the decay curves of the ground state (upper figure) and isomer (lower figure) α decay lines of ^{156}Hf, both of which are fitted with two components. The dashed line represents the random background from false correlations, while the dotted line is attributed to β decay feeding of these levels by the $\pi h_{11/2}$ level in ^{156}Ta and the solid line is the sum of these components. In both cases, the half-life deduced for the β decay feeding is consistent with that measured for the ^{156}Ta $\pi h_{11/2}$ proton decay line. The zero time difference in these decay curves corresponds to 393 ms for the ground state α decay line and 66 ms for the isomer α decay, respectively.

branches from ^{160}Re leading to ^{155}Hf. This is consistent with the decays proceeding between the same initial and final levels.

A long-lived component ($t_{1/2}>10$ ms) was observed by Hofmann *et al.* in the decay curve of the ^{156}Hf high-spin isomer and was interpreted as feeding of this level by favored Gamow-Teller β decays of the $\pi h_{11/2}$ level in ^{156}Ta [28]. Figure 11 shows the tails of the decay curves for both the ground state and isomer α decays of ^{156}Hf. In both cases the curves have been fitted with two components: The longer-lived component represents the random background rate for those decay events which are not successfully correlated with the true parent ion while the shorter-lived component is attributed to β decay feeding of the respective levels. In both cases the β decay feeding half-life deduced from the decay curves is consistent with the half-life measured for the ^{156}Ta $\pi h_{11/2}$ proton decay line.

A total yield of $\sim$3300 ^{156}Ta nuclei was deduced from the proton decay lines and fits to these decay curves, assuming 100% branching ratios for both ^{156}Hf α decay lines. For the $\pi h_{11/2}$ level the proton decay branching ratio was determined as 4.2 ± 0.9 % while the β decay feeding was found to be 56.4 ± 16.0 % to the ^{156}Hf ground state and 39.4 ± 12.8 % to the high-spin isomer. If the β decay to the isomeric state only feeds this level directly and is followed by the α decay, the above branching ratio would imply a logft value of 4.4 ±0.3, assuming a Q_{ec} value of 9.73 ± 0.95 [65] after correcting for the excitation energies of the initial and final states. This corresponds to a reduced Gamow-Teller transition probability of $0.18^{+0.17}_{-0.08}$ which is significantly lower than that measured for the corresponding transition in ^{154}Lu [66]. It is worth noting that with the present half-life measurement for the $\pi h_{11/2}$ level in ^{156}Ta, this general conclusion would not be significantly altered by an increased value for the β decay branching ratio to the ^{156}Hf isomer. Even if the branching ratio were 100%, the logft value would only drop to 4.0 ±0.2, with a corresponding transition probability of $0.46^{+0.31}_{-0.20}$. The partial proton decay half-life deduced from the present measurements for the 1108 keV ^{156}Ta proton decay line is 8.9 ± 2.3 s, which compares well with a value of 7.1 ± 1.6 s calculated in the WKB approximation with the Becchetti-Greenlees optical model potential [67] assuming a $h_{11/2}$ proton orbital.

A proton decay branch from ^{157}Ta was previously searched for the reaction 300 MeV ^{58}Ni + ^{106}Cd, leading to an upper limit of $\sim$1% for the proton decay branching ratio [1]. In the 290 MeV ^{58}Ni + ^{102}Pd reaction, approximately 5000 ^{157}Ta α decays were observed ($\sim$35 times more than in Ref. [1]), and so these data were analyzed to search for low-energy $A=157$ events correlated with ^{156}Hf α decays. A single candidate event with an energy of 919 ± 17 keV occurring 11 ms after ion implantation and followed 30 ms later by a 5878 ± 15 keV decay event was identified. Although this event sequence would be entirely consistent with a proton decay of ^{157}Ta followed by the α decay of ^{156}Hf, further experiments will be required to confirm whether this is the case. In particular, it is entirely possible that even if the observed event is a ^{157}Ta proton decay, it could be that the proton escaped from the DSSSD without depositing its full energy.

J. Gamma-ray coincidences

A high-efficiency germanium γ-ray detector was used to measure the energies of γ rays emitted in coincidence with decay events registered in the DSSSD. However, only in reaction 354 MeV ^{70}Ge + ^{106}Cd were statistically significant peaks observed, at energies of 92 keV and 162 keV. These γ-ray lines occurred in coincidence with the α decays of ^{171,172}Ir, respectively, in agreement with the conclusions of Schmidt-Ott *et al.* [47]. In Ref. [47], the mass assignments were based on an excitation function analysis and are confirmed in the present work using the direct mass information provided by the RMS.

IV. SUMMARY

The results of α decay measurements from 74 nuclides have been presented, including 8 new decay lines plus first measurements of 6 half-lives and 2 branching ratios. The unified energy calibration used in the present work is valid for both protons and α particles and complements the recently published survey of decay lines in the other region of proton and α radioactivity above ^{100}Sn [68,69]. The decay of a high-spin isomer in ^{157}Ta has been identified, completing a sequence of four α-emitting isomers in $N=84$ isotones and new fine structure has been observed for neutron-deficient tantalum and iridium isotopes. A challenge for future experiments will be to determine the relative energies of the α-emitting levels to learn more about proton single-particle energies in this region. New decay measurements of the proton radioactivity of ^{156}Ta have also been presented. The rich variety of spectroscopic information determined for such a wide range of nuclides serves to demonstrate the unique sensitivity and efficacy of implantation detection systems combined with recoil separators.

ACKNOWLEDGMENTS

The authors are indebted to the NSF operators for providing excellent beams and the laboratory staff for their technical support throughout this experimental program. R.D.P. and K.L. would like to acknowledge financial support from EPSRC and K.L. acknowledges additional financial support from Micron Semiconductor Limited.

[1] R.D. Page, P.J. Woods, R.A. Cunningham, T. Davinson, N.J. Davis, S. Hofmann, A.N. James, K. Livingston, P.J. Sellin, and A.C. Shotter, Phys. Rev. Lett. **68**, 1287 (1992).

[2] P.J. Sellin, P.J. Woods, T. Davinson, N.J. Davis, K. Livingston, R.D. Page, A.C. Shotter, S. Hofmann, and A.N. James, Phys. Rev. C **47**, 1933 (1993).

[3] P.J. Sellin, P.J. Woods, T. Davinson, N.J. Davis, A.N. James, K. Livingston, R.D. Page, and A.C. Shotter, Z. Phys. A **346**, 323 (1993).

[4] K. Livingston, P.J. Woods, T. Davinson, N.J. Davis, S. Hofmann, A.N. James, R.D. Page, P.J. Sellin, and A.C. Shotter, Phys. Lett. B **312**, 46 (1993).

[5] K. Livingston, P.J. Woods, T. Davinson, N.J. Davis, S. Hofmann, A.N. James, R.D. Page, P.J. Sellin, and A.C. Shotter, Phys. Rev. C **48**, R2151 (1993).

[6] K. Livingston, P.J. Woods, T. Davinson, N.J. Davis, A.N. James, R.D. Page, P.J. Sellin, and A.C. Shotter, Phys. Rev. C **48**, 3113 (1993).

[7] P.J. Sellin, P.J. Woods, D. Branford, T. Davinson, N.J. Davis, D.G. Ireland, K. Livingston, R.D. Page, A.C. Shotter, S. Hofmann, R.A. Hunt, A.N. James, M.A.C. Hotchkis, M.A. Freer, and S.L. Thomas, Nucl. Instrum. Methods Phys. Res. A **311**, 217 (1992).

[8] S. Hofmann, W. Faust, G. Münzenberg, W. Reisdorf, P. Armbruster, K. Güttner, and H. Ewald, Z. Phys. A **291**, 53 (1979).

[9] W.N. Lennard, S.Y. Tong, G.R. Massoumi, and L. Wong, Nucl. Instrum. Methods Phys. Res. B **45**, 281 (1990).

[10] S. Hofmann, G. Münzenberg, K. Valli, F.P. Hessberger, J.R.H. Schneider, P. Armbruster, B. Thuma, and Y. Eyal, GSI Scientific Report No. GSI-82-1, 1981, p. 241.

[11] W.N. Lennard, H. Geissel, K.B. Winterbon, D. Phillips, T.K. Alexander, and J.S. Forster, Nucl. Instrum. Methods Phys. Res. A **248**, 454 (1986).

[12] M.E. Leino, S. Yashita, and A. Ghiorso, Phys. Rev. C **24**, 2370 (1981).

[13] S. Hofmann, in *Particle Emission From Nuclei*, edited by D.N. Poenaru and M. Ivascu (CRC Press, Boca Raton, FL, 1989), Vol. 2, Chap. 2.

[14] A. Rytz, At. Data Nucl. Data Tables **47**, 205 (1991).

[15] B. Singh, Nucl. Data Sheets **73**, 490 (1994).

[16] J.D. Bowman, R.E. Eppley, and E.K. Hyde, Phys. Rev. C **25**, 941 (1982).

[17] B. Singh, Nucl. Data Sheets **55**, 348 (1988).

[18] E. Hagberg, P.G. Hansen, J.C. Hardy, P. Hornshoj, B. Jonson, S. Mattsson, and P. Tidemand-Petersson, Nucl. Phys. **A293**, 1 (1977).

[19] D. Schardt, R. Barden, R. Kirchner, O. Klepper, A. Plochocki, E. Roeckl, P. Kleinheinz, M. Piiparinen, B. Rubio, K. Zuber, C.F. Liang, P. Paris, A. Huck, G. Walter, G. Marguier, H. Gabelmann, and J. Blomqvist, in *Proceedings of the 5th International Conference on Nuclei Far From Stability*, Rosseau Lake, Canada, 1987, AIP Conference Proceedings 164 (American Institute of Physics, New York, 1988), p. 477.

[20] M.O. Kortelahti, K.S. Toth, K.S. Vierinen, J.M. Nitschke, P.A. Wilmarth, R.B. Firestone, R.M. Chasteler, and A.A. Shihab-Eldin, Phys. Rev. C **39**, 636 (1989).

[21] R.L. Mlekodaj, E.H. Spejewski, K.S. Toth, and Y.A. Ellis-Akovali, Phys. Rev. C **27**, 1182 (1983).

[22] K.S. Toth, K.S. Vierinen, M.O. Kortelahti, D.C. Sousa, J.M. Nitschke, and P.A.Wilmarth, Phys. Rev. C **44**, 1868 (1991).

[23] K.S. Vierinen, A.A. Shihab-Eldin, J.M. Nitschke, P.A. Wilmarth, R.M. Chasteler, R.B. Firestone, and K.S. Toth, Phys. Rev. C **38**, 1509 (1988).

[24] K.S. Toth, R.L. Hahn, C.R. Bingham, M.A. Ijaz, and R.F. Walker, Jr., Phys. Rev. C **7**, 2010 (1973).

[25] G.D. Alkhazov, L.K. Batist, E.Y. Berlovich, Y.S. Blinnikov, Y.V. Yelkin, K.A. Mezilev, Y.N. Novikov, V.N. Pantelejev, A.G. Polyakov, N.D. Shchigolev, V.N. Tarasov, V.P. Afanasjev, K.Y. Gromov, M. Jachim, M. Janicki, V.G. Kalinnikov, J. Kormicki, A. Potempa, E. Rurarz, F. Tarkanyi, and Y.V. Yushkevich, Z. Phys. A **291**, 397 (1979).

[26] K.S. Toth, K.S. Vierinen, J.M. Nitschke, P.A. Wilmarth, and R.M. Chasteler, Z. Phys. A **340**, 343 (1991).

[27] E. Hagberg, X.J. Sun, V.T. Koslowsky, H. Schmeing, and J.C. Hardy, Phys. Rev. C **45**, 1609 (1992).

[28] S. Hofmann, P. Armbruster, G. Berthes, T. Faestermann, A. Gillitzer, F.P. Hessberger, W. Kurcewicz, G. Münzenberg, K. Poppensieker, H.J. Schött, and I. Zychor, Z. Phys. A **333**, 107 (1989).

[29] S. Hofmann, G. Münzenberg, F.P. Hessberger, W. Reisdorf, P. Armbruster, and B. Thuma, Z. Phys. A **299**, 281 (1981). See also S. Hofmann, G. Münzenberg, W. Faust, F.P. Hessberger, W. Reisdorf, J.R.H. Schneider, P. Armbruster, K. Güttner, and B. Thuma, in Proceedings of the 4th International Conference on Nuclei Far from Stability, Helsingor, Denmark, 1981, edited by P.G. Hansen and O.B. Nielsen, CERN Report No. CERN 89-09, 1981 (unpublished), p. 190.

[30] C. Cabot, S. Della Negra, C. Deprun, H. Gauvin, and Y. Le Beyec, Z. Phys. A **287**, 71 (1978).

[31] E. Runte, T. Hild, W.-D. Schmidt-Ott, U.J. Schrewe, P. Tidemand-Petersson, and R. Michaelsen, Z. Phys. A **324**, 119 (1986).

[32] D.A. Eastham and I.S. Grant, Nucl. Phys. **A208**, 119 (1973).

[33] K.S. Toth, W.-D. Schmidt-Ott, C.R. Bingham, and M.A. Ijaz, Phys. Rev. C **12**, 533 (1975).

[34] U.J. Schrewe, W.-D. Schmidt-Ott, R.-D. v. Dincklage, E. Georg, P. Lemmertz, H. Jungclas, and D. Hirdes, Z. Phys. A **288**, 189 (1978).

[35] S. Della Negra, C. Deprun, D. Jacquet, and Y. Le Beyec, Ann. Phys. (Paris) **7**, 149 (1982).

[36] F. Meissner, H. Salewski, W.-D. Schmidt-Ott, U. Bosch-Wicke, and R. Michaelsen, Z. Phys. A **343**, 283 (1992).

[37] J. Borggreen and E.K. Hyde, Nucl. Phys. **A162**, 407 (1971).

[38] T. Hild, W.-D. Schmidt-Ott, V. Kunze, F. Meissner, C. Wennemann, and H. Grawe, Phys. Rev. C **51**, 1736 (1995).

[39] K.S. Toth, R.L. Hahn, M.A. Ijaz, and R.F. Walker, Jr., Phys. Rev. C **5**, 2060 (1972).

[40] E. Hagberg, P.G. Hansen, P. Hornshoj, B. Jonson, S. Mattsson, and P. Tidemand-Petersson, Nucl. Phys. **A318**, 29 (1979).

[41] H.A. Enge, M. Salomaa, A. Sperduto, J. Ball, W. Schier, Arnfinn Graue, and Arne Grauer, Phys. Rev. C **25**, 1830 (1982).

[42] U.J. Schrewe, E. Hagberg, H. Schmeing, J.C. Hardy, V.T. Koslowsky, and K.S. Sharma, Z. Phys. A **315**, 49 (1984).

[43] V.S. Shirley, Nucl. Data Sheets **64**, 627 (1991).

[44] C. Cabot, S. Della Negra, C. Deprun, H. Gauvin, and Y. Le Beyec, Z. Phys. A **283**, 221 (1977).

[45] P.J. Sellin, P.J. Woods, R.D. Page, S.J. Bennett, R.A. Cunningham, M. Freer, B.R. Fulton, M.A.C. Hotchkis, and A.N. James, Z. Phys. A **338**, 245 (1991).

[46] A. Siivola, Nucl. Phys. **A92**, 475 (1967).

[47] W.-D. Schmidt-Ott, H. Salewski, F. Meissner, U. Bosch-Wicke, P. Koschel, V. Kunze, and R. Michaelsen, Nucl. Phys. **A545**, 646 (1992).

[48] J.G. Keller, K.-H. Schmidt, F.P. Hessberger, G. Münzenberg, W. Reisdorf, H.-G. Clerc, and C.-C. Sahm, Nucl. Phys. **A452**, 173 (1986).

[49] J.R.H. Schneider, Report No. GSI-84-3, 1984.

[50] H. Gauvin, R.L. Hahn, Y. Le Beyec, M. Lefort, and J. Livet, Nucl. Phys. **A208**, 360 (1973).

[51] P.G. Hansen, H.L. Nielsen, K. Wilsky, M. Alpsten, M. Finger, A. Lindahl, R.A. Naumann, and O.B. Nielsen, Nucl. Phys. **A148**, 249 (1970).

[52] S. Della Negra, C. Deprun, D. Jacquet, and Y. Le Beyec, Z. Phys. A **300**, 251 (1981).

[53] C. Baglin, Nucl. Data Sheets **72**, 747 (1994).

[54] A. Siivola, Nucl. Phys. **A109**, 231 (1968).

[55] C. Cabot, C. Deprun, H. Gauvin, B. Lagarde, Y. Le Beyec, and M. Lefort, Nucl. Phys. **A241**, 341 (1975).

[56] J.R.H. Schneider, S. Hofmann, F.P. Hessberger, G. Münzenberg, W. Reisdorf, and P. Armbruster, Z. Phys. A **312**, 21 (1983).

[57] E. Browne, Nucl. Data Sheets **71**, 173 (1994).

[58] P.G. Hansen, B. Jonson, J. Zylicz, M. Alpsten, A. Appelqvist, and G. Nyman, Nucl. Phys. **A160**, 445 (1971).

[59] F.P. Hessberger, S. Hofmann, G. Münzenberg, W. Reisdorf, J.R.H. Schneider, and P. Armbruster, GSI Report No. GSI-82-1, 1982, p. 64.

[60] K.S. Toth, P.A. Wilmarth, J.M. Nitschke, R.B. Firestone, K. Vierinen, M.O. Kortelahti, and F.T. Avignone III, Phys. Rev. C **38**, 1932 (1988).

[61] R.B. Firestone, J.M. Nitschke, P.A. Wilmarth, K. Vierinen, J. Gilat, K.S. Toth, and Y.A. Akovali, Phys. Rev. C **39**, 219 (1989).

[62] M. Lewandowski, A.W. Potempa, V.I. Fominikh, K.Ya. Gromov, M. Janicki, Ju.V. Juschkevich, V.G. Kalinnikov, N.Ju. Kotovskij, V.V. Kuznetsov, N. Raschkova, Ja.A. Sajdimov, and J. Wawryszczuk, Z. Phys. A **340**, 107 (1991).

[63] K.S. Toth and W. Nazarewicz, Phys. Rev. C **48**, R978 (1993).

[64] J.O. Rasmussen, Phys. Rev. **113**, 1593 (1959).

[65] G. Audi and A.H. Wapstra, Nucl. Phys. **A565**, 66 (1993).

[66] W. Habenicht, L. Spanier, G. Korschinek, H. Ernst, and E. Nolte, in Proceedings of the 7th International Conference on Atomic Masses and Fundamental Constants, Darmstadt, Germany, 1984, edited by O. Klepper [THD-Schriftenreihe, Wissenschaft und Technik **26**, 244 (1984)].

[67] F.D. Becchetti, Jr. and G.W. Greeenlees, Phys. Rev. **182**, 1190 (1969).

[68] R.D. Page, P.J. Woods, R.A. Cunningham, T. Davinson, N.J. Davis, A.N. James, K. Livingston, P.J. Sellin, and A.C. Shotter, Phys. Rev. Lett. **72**, 1798 (1994).

[69] R.D. Page, P.J. Woods, R.A. Cunningham, T. Davinson, N.J. Davis, A.N. James, K. Livingston, P.J. Sellin, and A.C. Shotter, Phys. Rev. C **49**, 3312 (1994).